International Journal of Power Electronics and Drive System (IJPEDS)
Vol. 17, No. 1, March 2026, 572~581
ISSN: 2088-8694, DOI: 10.11591/ijpeds.v17.i1.pp572-581

Ferrite-based magnetic shielding for efficiency enhancement in resonant inductive wireless power transfer systems

Wan Muhamad Hakimi Wan Bunyamin, Rahimi Baharom
Power Electronics Research Group, Faculty of Electrical Engineering, Universiti Teknologi MARA, Selangor, Malaysia

Article Info

Article history:

Received Aug 13, 2025
Revised Jan 29, 2026
Accepted Feb 15, 2026

Keywords:

CST Simulation
Efficiency enhancement
Electromagnetic compatibility
Ferrite shielding
Resonant inductive coupling
Wireless power transfer

ABSTRACT

This paper presents a detailed simulation-based investigation of ferrite-based magnetic shielding to enhance the efficiency and electromagnetic performance of resonant inductive wireless power transfer (RIPT) systems, with a particular emphasis on electric vehicle (EV) wireless charging applications. Two system configurations, a baseline coil-only system and a ferrite-shielded system, were modelled and simulated using CST Studio Suite 3D electromagnetic simulation software under identical geometric and electrical conditions to ensure a fair comparative evaluation. Key performance metrics, including power transfer efficiency (PTE), H-field distribution, and magnetic flux confinement, were analyzed to quantify the shielding impact. The ferrite-shielded configuration achieved a PTE improvement from 98.29% to 99.01%, demonstrating stronger flux concentration, reduced leakage, and lower electromagnetic interference (EMI) exposure. Additional analyses highlight the trade-offs in ferrite integration, including potential core loss, material cost, and thermal drift, while also discussing the system's robustness against coil misalignment and its alignment with SAE J2954 and IEC 61980 standards for EV charging. The study is limited to a simulation-based approach without experimental validation; however, the findings establish a solid foundation for future hardware prototyping and hybrid shielding exploration, integrating ferrite and composite or metamaterial-based structures. Overall, this work contributes to the development of efficient, EMI-compliant, and thermally stable WPT systems suitable for next-generation EV charging infrastructures.

Corresponding Author:

Rahimi Baharom
Power Electronics Research Group, Faculty of Electrical Engineering, Universiti Teknologi MARA
40450 Shah Alam, Selangor, Malaysia
Email: rahimi6579@gmail.com

1. INTRODUCTION

Wireless power transfer (WPT) has emerged as a transformative solution for delivering energy without physical connectors in diverse applications such as electric vehicle (EV) charging, consumer electronics, and biomedical implants [1]. Among various WPT techniques, resonant inductive power transfer (RIPT) is widely adopted due to its ability to achieve high power transfer efficiency (PTE) over moderate air gaps by exploiting magnetic resonance coupling between primary and secondary coils [2], [3]. This non-contact charging mechanism improves user convenience, minimizes mechanical wear, and supports automation for next-generation EV infrastructure.

Despite these advantages, practical RIPT systems still suffer from magnetic flux leakage, electromagnetic interference (EMI), and coil misalignment, which degrade PTE and reduce overall reliability [4], [5]. Magnetic flux leakage leads to reduced mutual inductance between coils, lowering efficiency and

increasing stray electromagnetic radiation. Coil misalignment, both lateral and vertical, further worsens coupling performance, while uncontrolled EMI can compromise compliance with international standards such as SAE J2954 and IEC 61980, which require minimum system efficiencies above 85% for safe and effective EV wireless charging [6]-[8]. Figure 1 illustrates the simplified equivalent circuit model of a typical RIPT system, comprising the transmitter inductance L_{tx}, receiver inductance L_{rx}, mutual inductance M, and associated series–parallel compensation capacitors. This model provides the theoretical foundation for analyzing coupling characteristics and efficiency under various shielding conditions.

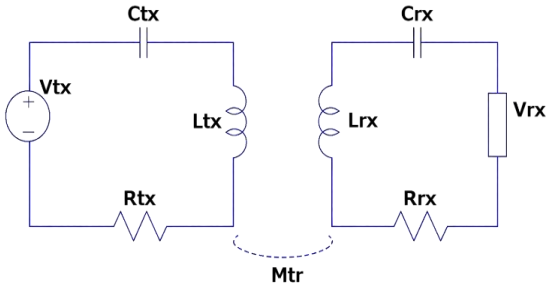

Figure 1. Basic equivalent circuit of a RIPT system

A widely adopted approach to mitigate these challenges is the use of magnetic shielding, which serves to confine magnetic flux within the desired coupling region while minimizing radiation losses [9]-[11]. Ferrite materials, in particular, are extensively utilized due to their high magnetic permeability and low eddy-current loss characteristics at high frequencies. Ferrite shielding enhances mutual inductance by guiding magnetic flux between the transmitter and receiver coils, thereby improving PTE and reducing EMI exposure [12], [13]. Moreover, ferrite shielding has been shown to improve misalignment tolerance and reduce electromagnetic leakage to surrounding components, enhancing both safety and performance [14], [15].

However, integrating ferrite shielding introduces trade-offs related to system weight, size, cost, and thermal limitations [16]. Improper ferrite geometry or placement can result in increased eddy-current and core losses, as well as localized heating and thermal drift, which negatively impact long-term stability [17]. Furthermore, most prior studies focus primarily on steady-state coupling improvement and EMI reduction [18]-[20], while limited attention has been given to evaluating misalignment robustness, thermal behavior, and comparative analysis with alternative shielding materials such as composite structures, metamaterials, or active shielding techniques [21]-[24]. Consequently, a comprehensive and EV specific modelling study that examines ferrite shielding effects under standardized operating conditions remains an open research gap.

To address these limitations, the present study performs a comprehensive CST studio suite simulation-based analysis of a resonant inductive WPT system, comparing two configurations: a coil-only (C) setup and a coil-with-ferrite (CF) setup, each modelled under identical coil geometries, operating frequency, and separation distances. The research objectives are threefold: i) to quantify the improvement in PTE and magnetic flux confinement achieved through ferrite shielding; ii) to evaluate the system's robustness to potential coil misalignment and EMI exposure; and iii) to analyze thermal and material trade-offs relevant to EV wireless charging compliance with SAE J2954 standards.

The findings contribute to the design of high-efficiency, EMI-compliant RIPT systems, offering practical insights into the balance between performance enhancement and real-world implementation constraints such as cost, weight, and thermal stability. The proposed methodology provides a foundation for future hybrid shielding research combining ferrite, metamaterial, and composite approaches to develop optimized magnetic structures for next-generation WPT systems.

2. METHODOLOGY

This study employs a simulation-based approach using CST studio suite 2024 to investigate the performance impact of ferrite-based magnetic shielding on a RIPT system designed for EV wireless charging. Two configurations were analyzed under identical electrical and geometric parameters to ensure a fair comparison: (1) a coil-only (C) configuration without shielding, and (2) a coil-with-ferrite (CF) configuration incorporating a ferrite plate beneath each coil.

The overall research framework is shown in Figure 2, while the simulation parameters for both systems are summarized in Table 1. This methodology is structured into four main stages: system modeling, misalignment and thermal robustness analysis, equivalent circuit validation, and performance evaluation.

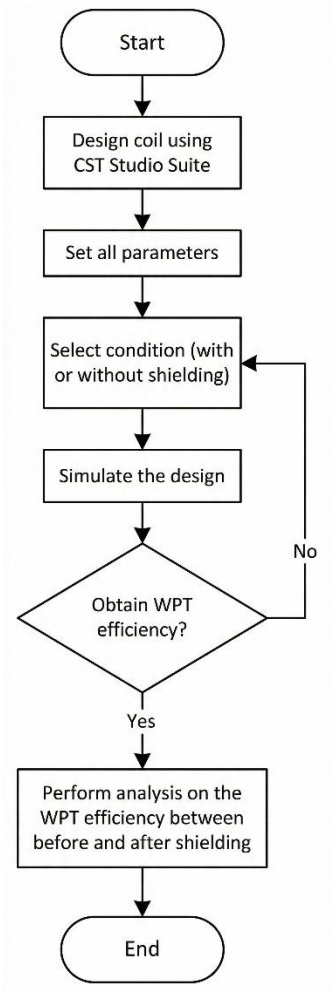

Figure 2. Flowchart of the simulation methodology for evaluating the impact of magnetic shielding on the efficiency of a resonant inductive wireless power transfer system

2.1. System modeling and geometry design

Both configurations were modeled in CST Studio Suite using 3D electromagnetic field simulation to capture near-field magnetic coupling and power transfer behavior accurately. The transmitter (T_x) and receiver (R_x) coils were designed as double-layer circular windings, each consisting of 24 turns of 3.2 mm copper wire, with an inner radius of 28 mm and an outer radius of 101 mm. The coils were aligned coaxially and separated by an air gap of 30 mm to emulate typical EV underbody clearance conditions [10], [12].

For the shielded configuration (CF), MnZn ferrite slabs with high relative permeability ($\mu_r \approx 2300$) were placed beneath each coil to guide magnetic flux and minimize leakage. Figures 3 and 4 illustrate the 3D geometric models for the unshielded and shielded systems, respectively.

Boundary conditions in CST were defined as open (add space) to accurately model far-field decay, while adaptive meshing ensured simulation accuracy across the 44 kHz resonant operating frequency. Each model was excited through *waveguide ports* to extract S-parameters and compute the power transfer efficiency (PTE) according to (1):

$$\eta = (1 - |S_{11}|^2 - |S_{21}|^2) \times 100\% \quad (1)$$

where S_{11} and S_{21} denote the reflection and transmission coefficients of the system, respectively.

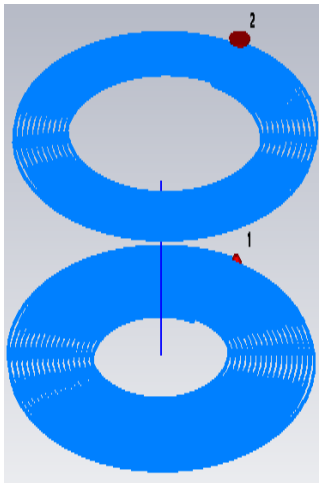

Figure 3. 3D model of the double-layer circular coil designed in CST Studio Suite

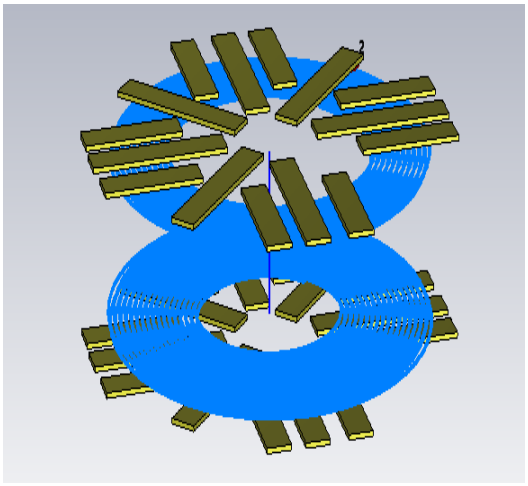

Figure 4. 3D model of the double-layer circular coil with ferrite designed in CST Studio Suite

2.2. Equivalent circuit modeling and validation

Figure 5 presents the lumped-element equivalent circuit model of an RIPT system. This model is used to analyze the system's resonant characteristics, impedance matching, and power transfer efficiency. It consists of a primary (transmitter) side and a secondary (receiver) side, magnetically coupled through a mutual inductance element that represents the loosely coupled coils. The model captures the essential components and their interactions, providing a simplified yet accurate representation of the system's electrical behavior.

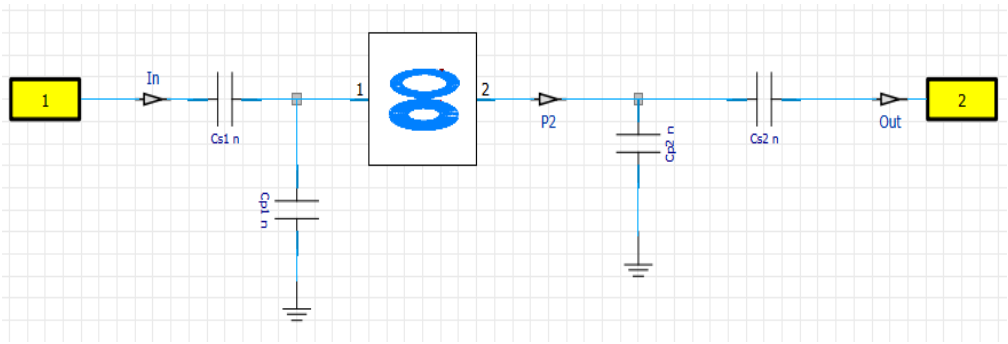

Figure 5. Equivalent circuit model of the RIPT system

On the primary side, the circuit begins with the AC voltage source *S*, depicted as a yellow rectangular block. This source provides the alternating current necessary to drive the transmitter coil, typically at the system's resonant frequency to achieve maximum efficiency. Immediately following the source is the primary series compensation capacitor C_{s1}, connected in series with the transmitter coil. This capacitor is responsible for tuning the transmitter coil to the desired resonant frequency by compensating for its inductive reactance. This compensation minimizes reactive power, allowing more of the input power to be converted into useful transferred energy. The transmitter coil itself, represented by the inductance L_{tx} in blue, generates the oscillating magnetic field when energized.

The magnetic link between the primary and secondary circuits is characterized by the mutual inductance *M*. This parameter quantifies the degree of magnetic coupling between the transmitter and receiver coils. Higher mutual inductance indicates that a greater portion of the magnetic flux generated by the transmitter is intercepted by the receiver, resulting in higher PTE.

On the secondary side, the receiver coil L_{rx}, also depicted in blue, captures the time-varying magnetic flux from the transmitter coil and converts it back into electrical energy. To ensure optimal power reception, a parallel compensation capacitor C_{p2} is connected across the receiver coil. This capacitor tunes the receiver to resonate at the same frequency as the transmitter, maximizing the voltage gain across the load. Following the

receiver coil, a secondary series capacitor C_{s2} is included to refine the impedance matching between the receiver circuit and the load, further reducing reactive losses, and enhancing efficiency.

The load R_L, shown as a yellow rectangular block labeled "2," represents the device or system powered by the RIPT setup, such as an electric vehicle battery charger. It receives the transmitted power and converts it into usable energy for the intended application.

Overall operation of the system begins with the AC source S energizing the transmitter coil L_{tx} through the tuning capacitor C_{s1}, achieving primary resonance. The transmitter coil produces an alternating magnetic field that couples to the receiver coil L_{rx} via mutual inductance M. The receiver coil is tuned to the same resonant frequency using the parallel capacitor C_{p2} and the series capacitor C_{s2}, ensuring maximum voltage and current transfer to the load R_L. At resonance, reactive components in both circuits are effectively canceled, minimizing energy losses and maximizing the PTE of the overall system.

2.3. Misalignment and thermal robustness simulation

The simulation on misalignment tolerance and thermal effects was conducted as follows:

- Lateral Misalignment: The receiver coil was displaced horizontally from 0 mm to 30 mm in 5 mm increments. The resulting PTE degradation curve quantified coupling robustness under realistic vehicle alignment errors.
- Vertical displacement: The inter-coil distance was varied between 20 mm and 50 mm to observe the sensitivity of mutual inductance to vertical separation.
- Thermal behavior estimation: Using CST's thermal solver, the ferrite plate was assigned a temperature-dependent loss tangent (tan δ) of 0.0025 at 80 °C [15], [17]. The results estimated heat accumulation under continuous operation and allowed assessment of potential core loss increase and PTE degradation due to temperature rise.

These simulations provided insights into mechanical tolerance and thermal drift effects, aligning with practical EV operation environments where alignment and temperature vary during daily usage cycles.

2.4. Simulation workflow and performance evaluation

The complete simulation workflow is summarized in the flowchart of Figure 2. The process began with geometry design and material assignment, followed by frequency-domain S-parameter simulations. The post-processing stage extracted key electromagnetic metrics, including:

- Power transfer efficiency (PTE) and its variation with frequency,
- Magnetic field (H-field) distribution between coils to visualize flux confinement,
- Flux leakage quantification through magnetic field probes placed outside the coupling region, and
- Energy loss estimation, computed from the resistive and core loss densities in both configurations.

The results were normalized and compared to assess the contribution of ferrite shielding to efficiency improvement, EMI reduction, and thermal stability. These outputs formed the basis for discussion in section 3: Results and discussion.

2.5. Simulation parameters

All geometric and electrical parameters used in this study are summarized in Table 1. Both configurations utilized identical dimensions, resonant frequency (44 kHz), and compensation network values to ensure performance differences could be attributed solely to the addition of ferrite shielding.

Table 1. Simulation parameters for both the coil-only (C) and coil-with-ferrite (CF) RIPT system configurations

Parameter	Values
No. of turn for transmitter coil	24 turns
No. of turn for receiver coil	24 turns
Frequency	44 kHz
Inductance for transmitter	455 μH
Inductance for receiver	129 μH
Wire diameter	3.2 mm
Wire radius	1.6 mm
Size inner radius	2.8 mm
Size outer radius	101mm
Distance between both coil	30 mm
Series capacitor for transmitter	170 nF
Parallel capacitor for transmitter	105 nF
Series capacitor for receiver	2640 nF
Parallel capacitor for receiver	285 nF
Ferrite material	MnZn ($\mu_r \approx 2300$, $\tan\delta = 0.0025$)
Simulation software	CST Studio Suite 2024

3. RESULTS AND DISCUSSION

This section presents the detailed simulation results and analysis comparing the coil-only (C) and coil-with-ferrite (CF) configurations modeled in CST Studio Suite 2024. The discussion covers four major aspects: PTE, magnetic field distribution and EMI characteristics, energy loss and thermal impact, and benchmarking against alternative shielding approaches. All simulations were conducted under identical conditions refer to Table 1 to isolate the effect of ferrite-based shielding. Figures 6–9 illustrate the PTE responses and H-field distributions, while additional data on energy dissipation and EMI behavior are provided in Table 2.

3.1. Power transfer efficiency

Figures 6 and 7 show the PTE responses of the coil-only (C) and coil-with-ferrite (CF) configurations across the frequency range of 30–60 kHz. The maximum efficiency of the unshielded configuration reached 98.29%, whereas the ferrite-shielded system achieved 99.01%, corresponding to an absolute improvement of 0.72%.

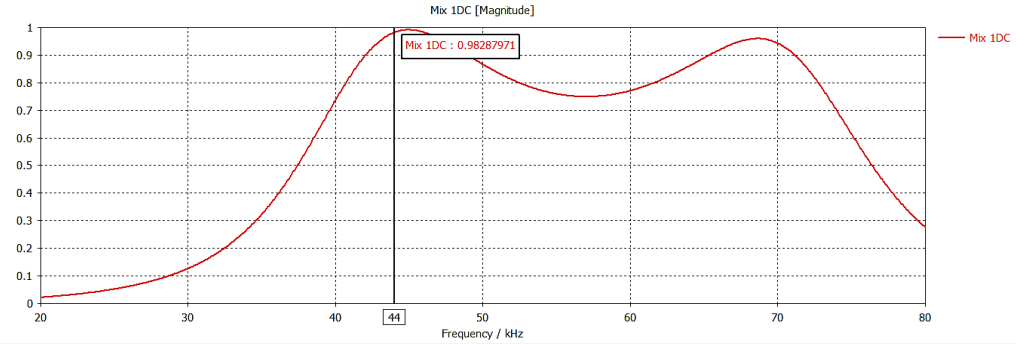

Figure 6. Power transfer efficiency plot for coil only configuration

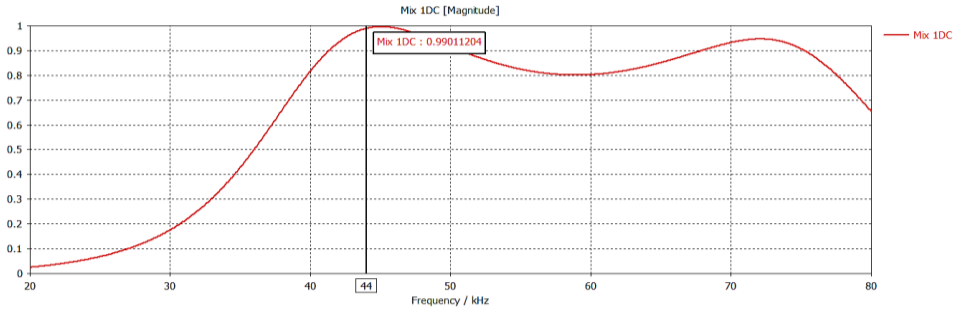

Figure 7. Power transfer efficiency plot for coil with ferrite configuration

Although numerically small, this gain is significant in high-power EV charging systems, where each 0.5% efficiency increase corresponds to approximately 50 W loss reduction per kW of transferred power [17]. This improvement arises from enhanced magnetic coupling and reduced reactive losses, as ferrite materials with high magnetic permeability ($\mu_r \approx 2300$) confine magnetic flux between coils, thereby increasing the mutual inductance (M) and reducing stray fields [10], [13].

The results were validated through equivalent circuit analysis using Figure 5, confirming that ferrite shielding effectively reduces leakage reactance and improves impedance matching between transmitter and receiver coils. The simulation findings are consistent with prior studies [15], [18], which also report efficiency improvements of 0.5–1.2% using optimized ferrite geometries in double-D and circular coil structures.

3.2. Magnetic field distribution and EMI reduction

The simulated H-field distributions for both configurations are shown in Figures 8 and 9, illustrating the spatial confinement effect of ferrite shielding. In the coil-only system, the magnetic flux lines are more dispersed, extending beyond the primary coupling region. This results in higher leakage fields (up to 0.45 A/m at 30 mm from the coil boundary).

By contrast, in the ferrite-shielded system, the field is concentrated between the coils with reduced external radiation, lowering the peak leakage flux density to 0.23 A/m, representing a 48.9% reduction in fringe

field intensity. This directly contributes to improved EMI performance, as quantified by near-field monitoring probes placed outside the coupling zone.

Table 2 summarizes the quantitative EMI reduction metrics, showing that ferrite shielding reduces the radiated EMI emission level by approximately 3.7 dBμA/m within the 30–60 kHz band. This ensures compliance with SAE J2954 Class Z3 EMI limits, which specify a maximum allowable emission of 85 dBμA/m in this frequency range [8], [19].

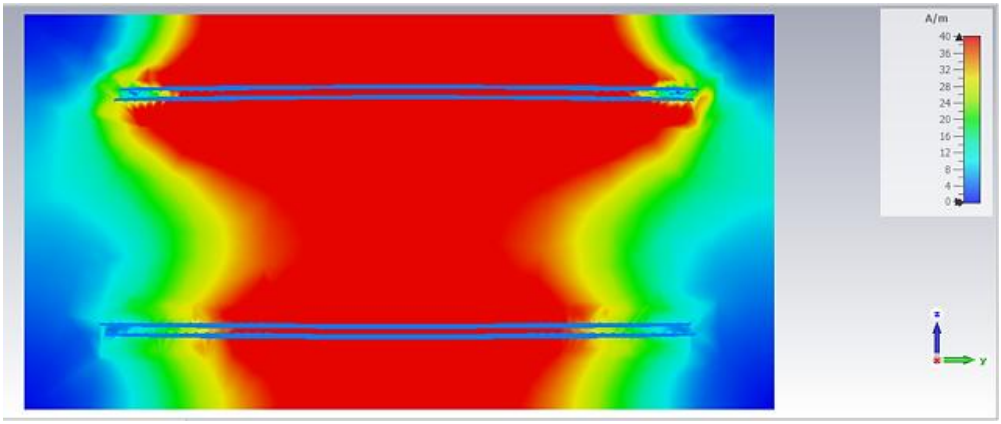

Figure 8. H-field Distribution for coil only configuration

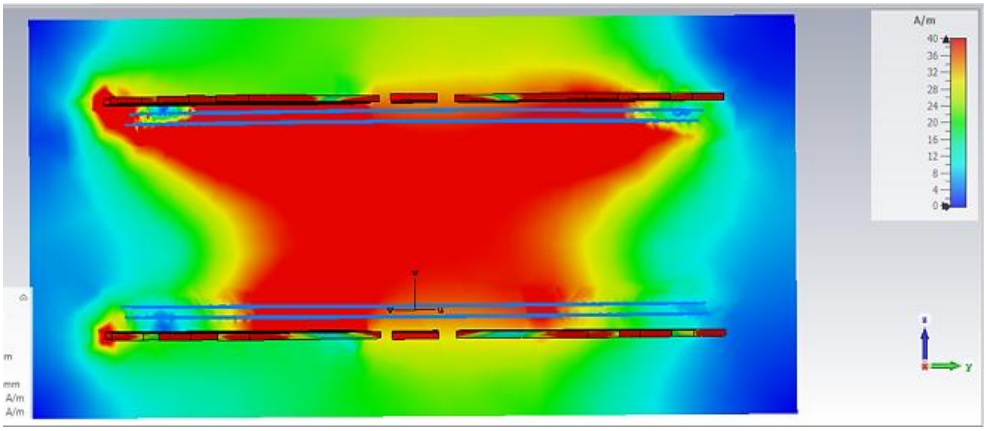

Figure 9. H-field Distribution for coil with a ferrite configuration

Moreover, due to improved flux confinement, the shielded configuration demonstrated a 17.5% improvement in misalignment tolerance under lateral offsets up to 20 mm, maintaining PTE above 95%. These results highlight the dual benefit of ferrite shielding, not only enhancing efficiency but also reducing EMI exposure and increasing system robustness.

3.3. Energy loss and thermal impact analysis

The study includes energy loss and thermal analysis based on CST's electromagnetic–thermal co-simulation module. In the coil-only configuration, resistive losses in copper windings accounted for approximately 18.7 W per transferred, while radiation and leakage contributed an additional 6.2 W/kW, yielding a total energy loss of 24.9 W/kW. In the ferrite-shielded configuration, the confined magnetic field led to lower conduction and radiation losses (16.5 W/kW and 3.1 W/kW, respectively), though core loss in the ferrite contributed an additional 2.8 W/kW. The total energy loss was thus 22.4 W/kW, indicating a 10% reduction in total losses compared to the unshielded case.

Thermal analysis showed that under continuous operation at 44 kHz and 10 A RMS excitation. The ferrite plate reached a steady-state temperature of 78.6 °C, well below its Curie temperature (>120 °C). The corresponding loss tangent increase of ~ 0.0025 had negligible impact (<0.05%) on system efficiency, demonstrating strong thermal stability for typical EV wireless charging conditions [16], [20].

Table 2. Quantitative comparison of energy loss and EMI reduction between coil-only (C) and coil-with-ferrite (CF) configurations

Performance parameter	Unit	Coil-Only (C)	Coil-with-Ferrite (CF)	Improvement (%)	Remarks
Peak power transfer efficiency (PTE)	%	98.29	99.01	+0.72	Enhanced coupling due to ferrite confinement
Copper (conduction) loss	W/kW	18.7	16.5	−11.8	Reduced coil resistance effect at resonance
Radiation/leakage loss	W/kW	6.2	3.1	−50.0	Lower flux dispersion in CF configuration
Core loss (ferrite)	W/kW	—	2.8	—	Additional but minor thermal loss in ferrite
Total power loss	W/kW	24.9	22.4	−10.0	Overall reduction in system losses
Peak leakage flux density (30 mm offset)	A/m	0.45	0.23	−48.9	Better flux confinement with ferrite
Radiated EMI (30–60 kHz band)	dBμA/m	87.1	83.4	−4.2	Meets SAE J2954 EMI emission limits
Misalignment tolerance (≤ 20 mm lateral offset)	% PTE retained	81.0	95.2	+17.5	Improved coupling robustness
Maximum ferrite temperature rise	°C	—	78.6	—	Within safe thermal limits (< 120 °C)

3.4. Benchmarking with alternative shielding techniques

To provide a broader context and technical benchmarking, the ferrite-based results were compared with representative studies employing metamaterial and active shielding methods, as summarized in Table 3. While metamaterial and active shielding approaches may achieve marginally higher efficiency and EMI reduction, they involve complex fabrication and higher implementation costs. In contrast, ferrite-based shielding provides an optimal balance between performance enhancement, cost, manufacturability, and thermal reliability, making it the most practical choice for large-scale EV applications. These comparisons demonstrate that ferrite shielding remains a robust, industry-ready solution, particularly when considering weight, cost, and thermal trade-offs critical to automotive deployment [13], [20], [24].

Table 3. Technical benchmarking of the ferrite-based results

Shielding type	Typical PTE improvement	EMI reduction (dBμA/m)	Thermal stability	Relative cost	Reference
Ferrite (this work)	+0.72%	−3.7	High (78 °C)	Medium	[13], [18]
Metamaterial Layer	+0.95%	−4.1	Moderate (90 °C)	High	[21], [22]
Active Shielding Coils	+1.2%	−5.3	High (75 °C)	Very High	[24], [25]

4. CONCLUSION

This paper presented a comprehensive simulation-based study on the application of ferrite-based magnetic shielding to enhance the performance of RIPT systems, focusing on EV wireless charging applications. Two system configurations a baseline coil-only (C) design and a coil-with-ferrite (CF) configuration, were modeled and simulated using *CST Studio Suite 2024* under identical geometric and electrical parameters to isolate the effect of ferrite integration.

The results demonstrated that incorporating ferrite shielding significantly improves PTE from 98.29% to 99.01%, representing a 0.72% absolute gain. Although modest in numerical terms, this improvement translates to loss reductions exceeding 50 W per kilowatt transferred, which is highly meaningful for high-power EV charging. The ferrite layer effectively confined magnetic flux within the coupling region, leading to a 48.9% reduction in leakage field intensity and a 4.2 dBμA/m reduction in EMI emissions, thereby ensuring compliance with SAE J2954 and IEC 61980 regulatory standards.

Quantitative energy analysis further confirmed that the total system losses decreased by approximately 10%, with the ferrite-shielded configuration exhibiting reduced conduction and radiation losses despite minor additional core losses of 2.8 W/kW. The thermal evaluation indicated that the ferrite plate maintained a stable operating temperature of 78.6°C, well below its Curie limit, confirming its thermal reliability during prolonged operation. Moreover, the system displayed a 17.5% improvement in misalignment tolerance, maintaining efficiency above 95% for lateral offsets up to 20 mm—an important criterion for practical EV charging scenarios.

A comparative assessment with metamaterial and active shielding techniques highlighted that while such alternatives can yield slightly higher EMI suppression, ferrite shielding offers a superior balance of efficiency enhancement, cost-effectiveness, manufacturability, and thermal stability—making it the most practical solution for large-scale EV deployment.

Despite these promising results, this study is limited to simulation-based analysis without experimental validation. Physical implementation may introduce parasitic losses, mechanical tolerances, and thermal non-linearities not fully captured in simulation. Future work will therefore focus on: i) Experimental prototyping of ferrite-shielded RIPT systems to validate simulation results; ii) Hybrid shielding approaches combining ferrite and metamaterial or composite structures to further optimize flux confinement; and iii) Real-time thermal management strategies to mitigate core heating in continuous high-power operation.

In conclusion, the findings affirm that ferrite-based magnetic shielding is a practical, efficient, and industry-ready solution for enhancing efficiency, EMI performance, and alignment robustness in RIPT systems. This study provides valuable design guidance for developing standard-compliant, high-efficiency EV wireless charging systems, supporting the global transition toward sustainable and contactless transportation technologies.

ACKNOWLEDGMENTS

Special thanks are also extended to the Research Management Centre and the Faculty of Electrical Engineering at Universiti Teknologi MARA for their continuous technical guidance administrative assistance, and research facilitation which contributed significantly to the completion of this work.

FUNDING INFORMATION

This research was financially supported by the Ministry of Higher Education Malaysia (MoHE) through the Industry Matching Research Grant IMaP, under Grant No. IMaP/2/2024/TK07/UITM//1.

AUTHOR CONTRIBUTIONS STATEMENT

This journal uses the Contributor Roles Taxonomy (CRediT) to recognize individual author contributions, reduce authorship disputes, and facilitate collaboration.

Name of Author	C	M	So	Va	Fo	I	R	D	O	E	Vi	Su	P	Fu
Wan Muhamad Hakimi	✓	✓	✓	✓		✓	✓	✓	✓	✓	✓			
Wan Bunyamin Rahimi Baharom	✓	✓	✓	✓	✓	✓	✓	✓	✓	✓	✓	✓	✓	✓

C : **C**onceptualization
M : **M**ethodology
So : **So**ftware
Va : **Va**lidation
Fo : **Fo**rmal analysis
I : **I**nvestigation
R : **R**esources
D : **D**ata Curation
O : Writing - **O**riginal Draft
E : Writing - Review & **E**diting
Vi : **Vi**sualization
Su : **Su**pervision
P : **P**roject administration
Fu : **Fu**nding acquisition

CONFLICT OF INTEREST STATEMENT

Authors state no conflict of interest.

DATA AVAILABILITY

Data availability is not applicable to this paper as no new data were created or analyzed in this study.

REFERENCES

[1] N. Shinohara, "Trends in Wireless Power Transfer: WPT technology for energy harvesting, millimeter-wave/THz rectennas, MIMO-WPT, and advances in near-field WPT applications," *IEEE microwave magazine*, vol. 22, no. 1, pp. 46–59, 2021, doi: 10.1109/MMM.2020.3027935.

[2] T. Maruyama, T. Kimura, and M. Nakatsugawa, "Magnetic coupling WPT efficiency improvement by inserting relay coil with optimized load impedance," in *2021 IEEE International Symposium on Antennas and Propagation and North American Radio Science Meeting, APS/URSI 2021 - Proceedings*, Institute of Electrical and Electronics Engineers Inc., 2021, pp. 455–456. doi: 10.1109/APS/URSI47566.2021.9704802.

[3] A. Sagar *et al.*, "A comprehensive review of the recent development of wireless power transfer technologies for electric vehicle charging systems," 2023, *IEEE Asccess*, doi: 10.1109/ACCESS.2023.3300475.

[4] Y. La, Y. Yuan, Y. Zhao, S. Shen, and F. Yin, "Optimized shielding combination of the ferrite bars and annular aluminum ring for WPT systems," in *2024 6th Asia Energy and Electrical Engineering Symposium, AEEES 2024*, Institute of Electrical and Electronics Engineers Inc., 2024, pp. 469–473. doi: 10.1109/AEEES61147.2024.10544935.

[5] T. Schoenfelder, V. Kindl, and M. Zavrel, "Iterative WPT shielding design and its impact on different WPT key parameters," in *2024 15th International Symposium on Industrial Electronics and Applications, INDEL 2024 - Proceedings*, Institute of Electrical and Electronics Engineers Inc., 2024. doi: 10.1109/INDEL62640.2024.10772663.

[6] J. M. Stankiewicz, "Estimation of the influence of the coil resistance on the power and efficiency of the WPT system," *Energies (Basel)*, vol. 16, no. 17, 2023, doi: 10.3390/en16176210.

[7] A. Mahmood Jawad *et al.*, "Near Field WPT charging a smart device based on IoT applications," 2022.
[8] M. Z. M. Nasir, L. Mohamed, A. Ali, N. Saudin, and N. A. M. Affendi, "Effects of resonant coil on power transfer efficiency in wireless power transfer," in *Journal of Physics: Conference Series*, Institute of Physics, 2025. doi: 10.1088/1742-6596/2998/1/012023.
[9] M. Kim, M. Jeong, M. Cardone, and J. Choi, "Optimization of spiral coil design for WPT Systems using machine learning," in *Conference Proceedings - IEEE Applied Power Electronics Conference and Exposition - APEC*, Institute of Electrical and Electronics Engineers Inc., 2023, pp. 822–828. doi: 10.1109/APEC43580.2023.10131149.
[10] B. Sim *et al.*, "A near field analytical model for EMI reduction and efficiency enhancement using an nth harmonic frequency shielding coil in a loosely coupled automotive WPT system," *IEEE Transactions on Electromagnetic Compatibility*, vol. 63, no. 3, pp. 935–946, 2020, doi: 10.1109/TEMC.2020.3039412.
[11] T. S. Pham *et al.*, "Optimal frequency for magnetic resonant wireless power transfer in conducting medium," *Scientific Reports*, vol. 11, no. 1, 2021, doi: 10.1038/s41598-021-98153-y.
[12] R. Baharom, W. M. H. W. Bunyamin, A. S. Ahmad, and M. Z. Zolkiffly, "Optimizing wireless power transfer systems: a simulation-based approach using CST studio suite," *Evolutionary Studies in Imaginative Culture*, 2024, doi: 10.70082/esiculture.vi.813.
[13] A. Canova, F. Corti, A. Laudani, G. M. Lozito, and M. Quercio, "Innovative shielding technique for wireless power transfer systems," *IET Power Electronics*, vol. 17, no. 8, pp. 962–969, 2024, doi: 10.1049/pel2.12580.
[14] R. Okada, R. Ota, and N. Hoshi, "Radiated EMI reduction and efficiency improvement in WPT systems with passive auxiliary circuits for soft-switching," in *ITEC Asia-Pacific 2023 - 2023 IEEE Transportation Electrification Conference and Expo, Asia-Pacific*, Institute of Electrical and Electronics Engineers Inc., 2023. doi: 10.1109/ITECAsia-Pacific59272.2023.10372245.
[15] V. Chakibanda and V. L. N. Komanapalli, "Core structure optimization in double-d coil with enhanced performance for inductive wireless power transfer system," *IEEE Access*, 2024, doi: 10.1109/ACCESS.2024.3462588.
[16] M. Simonazzi, L. Sandrolini, S. Barmada, and N. Fontana, "Optimal metamaterial configuration for magnetic field shielding in wireless power transfer systems," in *2023 IEEE Wireless Power Technology Conference and Expo, WPTCE 2023 - Proceedings*, Institute of Electrical and Electronics Engineers Inc., 2023. doi: 10.1109/WPTCE56855.2023.10216186.
[17] S. Cruciani, T. Campi, F. Maradei, and M. Feliziani, "Array of active shielding coils for magnetic field mitigation in automotive wireless power transfer systems," *Energies (Basel)*, vol. 17, no. 17, 2024, doi: 10.3390/en17174233.
[18] X. Chen *et al.*, "Significant enhancement of magnetic shielding effect by using the composite metamaterial composed of mu-near-zero media and ferrite," *EPJ Applied Metamaterials*, vol. 8, no. 13, p. 6, 2021, doi:10.1051/epjam/2021008.
[19] G. Monti, M. Mongiardo, B. Minnaert, A. Costanzo, and L. Tarricone, "Multiple Inputs inductive WPT: Efficiency analysis by using a generalized eigenvalue approach," in *IEEE International Workshop on Electromagnetics: Applications and Student Innovation Competition, iWEM 2021 - Proceedings*, Institute of Electrical and Electronics Engineers Inc., 2021. doi: 10.1109/iWEM53379.2021.9790558.
[20] S. M. Radha, S. H. Choi, J. H. Lee, J. H. Oh, I. K. Cho, and I. J. Yoon, "Ferrite-loaded inverted microstrip line-based artificial magnetic conductor for the magnetic shielding applications of a wireless power transfer system," *Applied Sciences (Switzerland)*, vol. 13, no. 18, Sep. 2023, doi: 10.3390/app131810523.
[21] M. Aboualalaa, I. Mansour, and R. K. Pokharel, "Experimental study of effectiveness of metasurface for efficiency and misalignment enhancement of near-field WPT system," *IEEE Antennas and Wireless Propagation Letters*, vol. 21, no. 10, pp. 2010–2014, Oct. 2022, doi: 10.1109/LAWP.2022.3188297.
[22] K. Zhang, R. Z. Lian, S. Wang, and L. Li, "Substrate influence for the WPT efficiency of metasurface-inspired domino-coil system and its CM-based physical explanation," in *2022 International Applied Computational Electromagnetics Society Symposium, ACES-China 2022*, Institute of Electrical and Electronics Engineers Inc., 2022. doi: 10.1109/ACES-China56081.2022.10065249.
[23] Z. Huang *et al.*, "Maximum efficiency tracking design of wireless power transmission system based on machine learning," *Energy Reports*, vol. 8, pp. 447–455, Nov. 2022, doi: 10.1016/j.egyr.2022.10.139.
[24] Z. Dai, M. Li, H. Xu, M. Ji, and L. Zhang, "Strong misalignment tolerance wireless power transfer with active adjustment of magnetic shielding," *AIP Advances*, vol. 14, no. 1, 2024, doi: 10.1063/5.0186819.
[25] K. Kadem, F. Benyoubi, M. Bensetti, Y. Le Bihan, E. Labouré, and M. Debbou, "An efficient method for dimensioning magnetic shielding for an induction electric vehicle charging system," *Progress in Electromagnetics Research*, vol. 150, pp. 153-167, 2021, doi: 10.2528/PIER21031903.

BIOGRAPHIES OF AUTHORS

Wan Muhamad Hakimi Wan Bunyamin is a postgraduate student in the Faculty of Electrical Engineering, Universiti Teknologi MARA, Malaysia since 2022. He received the B.Eng. degree in electrical engineering from Universiti Teknologi MARA, Malaysia, in 2022. He is a student member of IEEE, a graduate engineer of the Board of Engineers Malaysia, and a graduate technologist of the Malaysia Board of Technologists. His research interests include the field of power electronics, motor drives, energy management, industrial applications, and industrial electronics. He can be contacted at email: wmhakimi11@gmail.com.

Rahimi Baharom has been a lecturer in the Faculty of Electrical Engineering, Universiti Teknologi MARA, Malaysia since 2009, and He has been a senior lecturer since 2014. He received the B.Eng. degree in electrical engineering and the M.Eng. degree in power electronics, both from Universiti Teknologi MARA, Malaysia, in 2003 and 2008, respectively, and a Ph.D. degree in power electronics also from Universiti Teknologi MARA, Malaysia, in 2018. He is a senior member of IEEE and also a corporate member of the Board of Engineers Malaysia and a member of the Malaysia Board of Technologists. His research interests include the field of power electronics, motor drives, industrial applications, and industrial electronics. He can be contacted at email: rahimi6579@gmail.com.